A Hybrid Intelligent Controlled DC-DC Converter for Photovoltaic energy system application

Seyyed Mehdi Mirebrahimi[1], Iman Soltani[2,*]

[1]Department of Electrical Engineering,Firoozkooh Branch,Islamic Azad university,Firoozkooh,Iran

mirebrahimi@iaufb.ac.ir

[2]Department of Electrical Engineering,Firoozkooh Branch,Islamic Azad university,Firoozkooh,Iran

I_soltani@ikiu.ac.ir

ABSTRACT

A photovoltaic (PV) power generation system under partial shaded conditions (PSC) exhibits multiple power peaks in the power-voltage (P-V) characteristic curve and traditional optimization methods fail to detect the global maximum power point (GMPP). This paper proposes a hybrid intelligent algorithm by combining particle swarm optimization with chaos searching technique (CSTPSO) to improve the maximum power point (MPP) tracking capability for PV system under partial shading condition. The key advantage of the proposed technique is the elimination of PI control loops using direct duty cycle control method. Furthermore, since the CSTPSO is based on optimized search method, it overcomes the common drawback of the conventional MPPT. Simulation results indicate that the proposed method outperforms others method in terms of global peak (GP) tracking speed and accuracy under various partial shading conditions. Furthermore , it is tested using data of a tropical cloudy day, which includes rapid movement of the passing clouds and partial shading.

KEYWORDS: DC-DC Power Convertors, Optimal Control, Photovoltaic Power Systems.

1. INTRODUCTION

Photovoltaic (PV) energy generation provides numerous advantages over the other renewable energy sources such as environmental friendliness, absence of rotating parts, ease of mounting on roof tops etc [1]. The recently introduced governmental laws and policies [2]-[3] make PV systems attractive and as a result the installation of PV arrays within urban locations is becoming increasingly widespread. One of the major challenges in the extraction of power rises from partial shading due to neighboring buildings, trees and passing clouds. To ensure the optimal utilization of large PV arrays, maximum power point tracker (MPPT) is employed in conjunction with the power converter (dc-dc converter and/or inverter). However, due to the varying environmental condition such as temperature and solar insolation, the P–V characteristics curve exhibit inconsistent maximum power point (MPP), posing a challenge to the tracking problem. The situation becomes more complicated when the array is subjected to partial shading, i.e. a condition when a part or the whole module of the PV array receives non-uniform insolation. During partial shading, the P–V curves are characterized by multiple peaks-several local and one global peak (*GP*). If the true *GP* is not properly tracked, the MPPT algorithm might be trapped at one of the local peak, with the consequence of significant power losses [8]. To date, various MPPT techniques have been proposed; amongst these, the hill

climbing (HC) [9], perturb and observe (P&O) [12] and incremental conductance (IC) [13] are the most widely used. Although these methods are quite simple to implement, they are incapable of handing the partial shading condition as they lacked the sufficient intelligence to differentiate between the local and global peak. Additionally, rapid fluctuations of solar insolation may cause the algorithm to lose track of the MPP direction completely .Several attempts have been carried out to improve these algorithms to cater for partial shading. In [12], a compensation method for a series-parallel (S-P) array is proposed. When shading occurs, it activates the corresponding bypass diodes of the PV module according to the shading level. Despite its effectiveness, the technique could only be applied to an array with the S-P configuration. Authors in [13] proposed a two-stage method to track the *GP*. In the first stage, the neighborhood of the *GP* is detected; the obtained information later becomes the basis for tracking the *GP* in the second stage. However, it was noted that the method fails to track the *GP* for all shading conditions. In another work [14], a critical study of I–V and P–V characteristics under the partial shading was carried out. Using the results of this study, The authors proposed a two mode tracking. First, a sudden change in operating power activates a subroutine that tracks all possible local MPPs. Then all the local peaks are evaluated to determine which one is the actual GP. The problem, however, is that for certain shading conditions, the algorithm needs to scan almost 80% of the I–V curve in order not to miss any potential peak that would become the GP. Consequently, the MPPT response is slow. In another work [26], a two mode dividing rectangle (DIRECT) search method in conjunction with the conventional P&O is proposed. A global mode is activated during partial shading and subsequently the DIRECT algorithm tries to track the *GP*. Once the stopping condition is achieved, it activates the P&O method to maintain the operating point at GP. Although, this method has been proven to be effective for most of the times, the algorithm is very complex; it increases the computation burden of the overall MPPT system significantly. Recently, several works are carried out to employ artificial intelligence technique, in particular the fuzzy logic control (FLC) for MPPT [16-18]. Although FLC MPP tracking is effective, it requires extensive processes which include fuzzification, rule base storage, inference mechanism and defuzzification operations. Consequently, compromise has to be made between tracking speed and computational cost. An alternative approach is to treat the MPP tracking as an optimization problem and thereafter applying the evolutionary algorithms (EA) to search for the global maxima. Due to its ability to handle multi-modal objective functions [19, 20], EA are envisaged to be well suited for a problem of such nature. Recognizing these advantages, various authors have employed particle swarm optimization (PSO) to track the GP during the partial shading [21-23]. However, in all these PSO methods, random numbers are used. The main disadvantage of this approach is that the randomness tends to reduce the searching efficiency significantly. For example, during the exploration process, if a low valued random number is multiplied with the present information of control variable (voltage, current or duty cycle), only a small change in the velocity term of the PSO equation is obtained. This small perturbation may be insufficient to bring the operating point to near the desired value. Consequently, further iterations need to be carried out. However, there is no guarantee that the random number in the subsequent iteration will close the gap towards the *GP*. On the other hand, if the perturbation is too large, it may cause the control variable to escape from the *GP* region and possibly being trapped into the vicinity of a local peak. Furthermore, the unpredictability of solution due to randomness is more severe if the number of particles is small. Increasing the number of particles will improve the chances of converging to a

feasible solution. However, this can only be achieved at the expense of computation time. If the time taken to locate the *GP* is too long, practical implementation of the algorithm may not be possible. In view of these drawbacks, this paper introduces a CSTPSO to improve the tracking capability of the conventional PSO algorithm. The main idea is to remove the random number in the accelerations factor of the PSO velocity equation. In addition, the maximum change in velocity, V_{max} , is restricted to a particular value– which will be determined based on the critical study of P–V characteristics during partial shading. *To* evaluate the idea, the algorithm is implemented on a boost converter and compared to the conventional MPPT methods. The proposed approach offers several advantages: (1) due to the absence of random values, the particles follow a deterministic behavior; for each independent run, the solution is consistent even with a small number of particles (2) only one parameter i.e. the inertia weight, need to be tuned, (3) the optimization structure is much simpler compared to conventional PSO and (4) by limiting V_{max} , the algorithm can be very useful in frequently changing environmental conditions.

2. NON-LINEAR CHARACTERISTICS OF PV ARRAY UNDER PARTIAL SHADED CONDITIONS

Fig.1 shows the model of a generalized S-P configuration of a PV array. The output current equation of this topology using two-diode model can be written as [24]:

$$I = I_{PV} - I_{o1}\left[\exp\left(\frac{V+IR_s}{a_1 V_{T1}}\right)-1\right] - I_{o2}\left[\exp\left(\frac{V+IR_s}{a_2 V_{T2}}\right)-1\right]-\left(\frac{V+IR_s}{R_p}\right) \quad (1)$$

Where

$$Id_1 = \exp\left(\frac{V+IR_s\Gamma}{V_T N_{ss}}\right) \quad (2)$$

$$Id_2 = \exp\left(\frac{V+IR_s\Gamma}{(p-1)V_T N_{ss}}\right) \quad (3)$$

$$p = 1 + a_2 \geq 2.2$$

$$\Gamma = \frac{N_{ss}}{N_{pp}} \quad (4)$$

where I_{PV} is the current generated by the incidence of light; I_o is the equivalent reverse saturation currents of diode1 and diode2, respectively. Other variables are defined as follows: V_T (N_s kT/q) is the thermal voltages of the PV module having N_s cells connected in series, q is the electron charge (1.60217646×10^{-19} C), k is the Boltzmann constant (1.3806503×10^{-23} J/K) and T is the temperature of the p-n junction in Kelvin. Variable a_2 represents the diode ideality constant. N_{ss} and N_{pp} are the series and parallel PV modules, respectively.

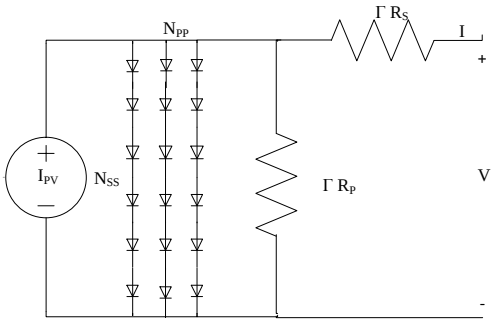

Fig. 1 Series parallel (S-P) combination of PV array.

Fig. 2 (a) shows a more practical arrangement of a PV array, in which two additional diodes are connected. First is the bypass diode that is connected in parallel with each PV module to protect modules from hot-spot. This problem usually occurs when a number of the series PV cells modules are less illuminated and behave as a load instead of a generator. In literature, this is known as partial shading. The second is the blocking diode connected at the end of each PV string. It protects the array from being affected by the current imbalance between the strings.

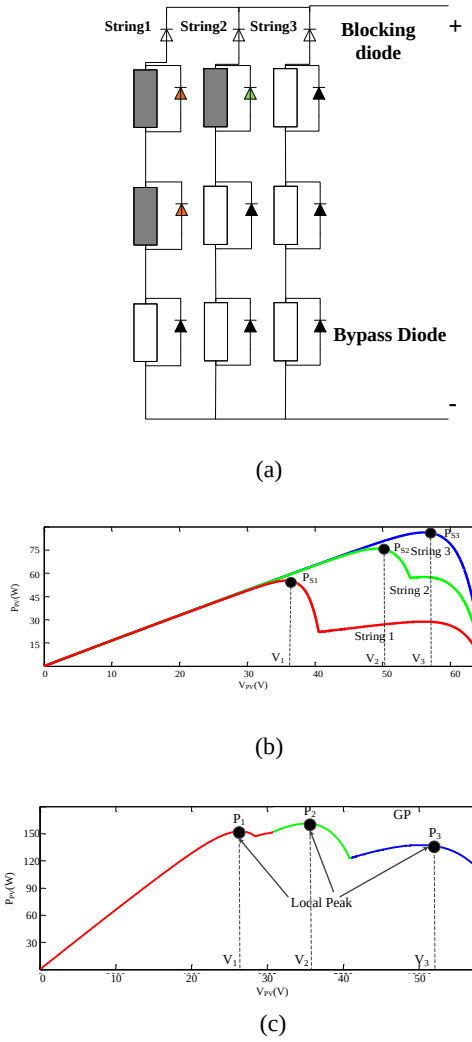

Fig.2. (a) Operation of PV array partial shading: For uniform irradiation, the module has solar insolation G=1000W/m^2, shaded module has G=500W/m^2(b) P–V curves for each string. (c) The resultant P–V curve for entire array

When the PV array is operating under uniform insolation, the resulting P–V characteristics curve of the array exhibit a single MPP. However, during partial shading, these additional diodes transform the P–V curves into more complicated shape–characterized by several local and one global peak. This effect can be visualized by an SP configuration comprises of three strings, each having three set of PV modules, as shown in Fig. 2 (a). In this figure, each module has a nominal rating of 25W at standard testing conditions (*STC*). When the PV array receives a uniform insolation of 1000W/m^2 (string 3), the parallel diodes are reverse biased; consequently the PV current flows due to the series PV modules. However, when PV array is subjected to partial shading (string 1 and 2), the shaded modules receives a reduced solar irradiance of 500W/m^2 . The voltage difference between the two unequally irradiated modules activates the bypass diode of the lower irradiated string. As a result, the resulting P–V curve for each shaded string is characterized by two peaks, namely PS_2 (60W) for string 2 and PS_1 (40W) for string 1 [14, 24]. By investigating Fig. 2(b), it can be noted that the peaks PS_1 , PS_2 and PS_3 occur at V_1=24 V, V_2=35 V, and V_3=52 V, respectively. The key point to note here is that each string exhibits its maximum peak at 80% of open circuit voltage (V_{oc}) of the unshaded modules. The resulting P–V curve for the entire array is shown in Fig. 2 (c). It can be observed that the position of PS_1 , PS_2 , and PS_3 govern the position of the peaks P_1 , P_2 and P_3 , correspondingly. Moreover, these Peaks occur nearly at the voltages V_1 , V_2 and V_3 ,respectively. Furthermore, it can be deduced that all the local peaks are displaced to each other by an integral multiple of 80% of V_{oc} (n×0.8×V_{oc}) of a single PV module, where "*n*" is an integer. Since the minimum integral difference in the number of shaded modules between the series modules of two strings is one, the minimum possible displacement between two successive peaks is 0.8×V_{oc}module. These important observations of partially shaded PV array is described in [14]. They will be used later in the implementation stage of the proposed MPPT method.

3. CONVENTIONAL PARTICLE SWARM OPTIMIZATION (PSO)

3.1. Brief introduction to PSO

Particle swarm optimization (PSO) is a stochastic, population-based EA search method, modeled after the behavior of bird flocks [32]. A PSO algorithm maintains a swarm of individuals (called particles), where each particle represents a candidate solution. Particles follow a simple behavior: emulate the success of

neighboring particles and its own achieved successes. The position of a particle is therefore influenced by the best particle in a neighborhood, P_{best} , as well as the best solution found by the particle itself, G_{best} . Particle position, x_i , are adjusted using:

$$x_i^{k+1} = x_i^k + v_i^{k+1} \tag{5}$$

where the velocity component, v_i , represents the step size. The velocity is calculated by:

$$v_i^{k+1} = w v_i^k + c_1 r_1 \left\{P_{besti} - x_i^k\right\} + c_2 r_2 \left\{G_{best} - x_i^k\right\} \tag{6}$$

where w is the inertia weight, c_1 and c_2 are the acceleration coefficients, r_1 , r_2 ϵ U (0,1), P_{besti} is the personal best position of particle$_i$, and G_{best} is the best position of the particles. Note that r_1 and r_2 are random numbers. Fig. 3 shows the typical movement of particles in the optimization process.

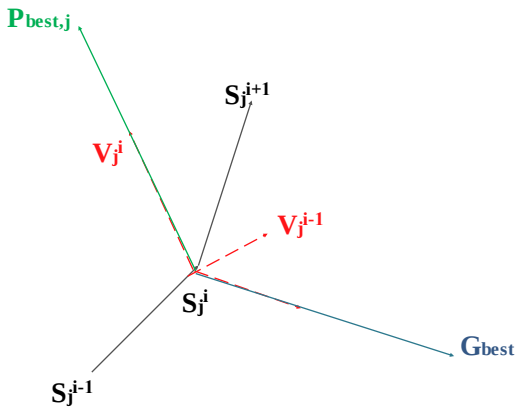

Fig. 3. Movement of particles in the optimization process[15]

3.2. Brief introduction to CST

Chaos is a kind of non periodic moving style. It exists widely in the nonlinear system and is unique to the system. It appears stochastic but can be generated through deterministic means. Chaos is a kind of unshaped out-of-order state, which blends with specific forms relative to some ‘‘immobile points’’,‘‘periodic points’’ [33]. Chaos has subtle internal structure and it is a kind of ‘‘strange attractor’’, which can attract the movement of system and confine it within the specified range. The chaos searching technique (CST) is a new kind of searching method [33]. The basic idea of the algorithm is to transform the variable of problems from the solution space to chaos space and then perform search to find out the solution by virtue of the random city, orderliness and ergodi city of the chaos variable. Chaos searching technique includes two steps: firstly, search all the points in turn within the changing range of variables and taking the better point as the current optimum point; then regard the current optimum point as the center, a tiny chaos disturbance is imposed and more careful search is performed to find out the optimum point. The chaos search technique has many advantages such as not sensitive to the initial value, easy to skip out of the locally minimum value, fast searching velocity and global gradual convergence. The following Logistic map is used to generate the chaos sequence because it is more convenient to use:

$$Z_{i+1} = \mu Z_i (1 - Z_i) \tag{7}$$

where $z_i \in [0,1]$ $(i = 1,2,...)$ is the chaos variable $i(i = 1,2,...)$ is the times of iteration; and μ is the control parameter. It is easy to testify that the system is entirely in chaos situation when $\mu = 4$ and the chaos space belongs to [0, 1]. The flow chart of the proposed algorithm is shown in the following Fig. 4.

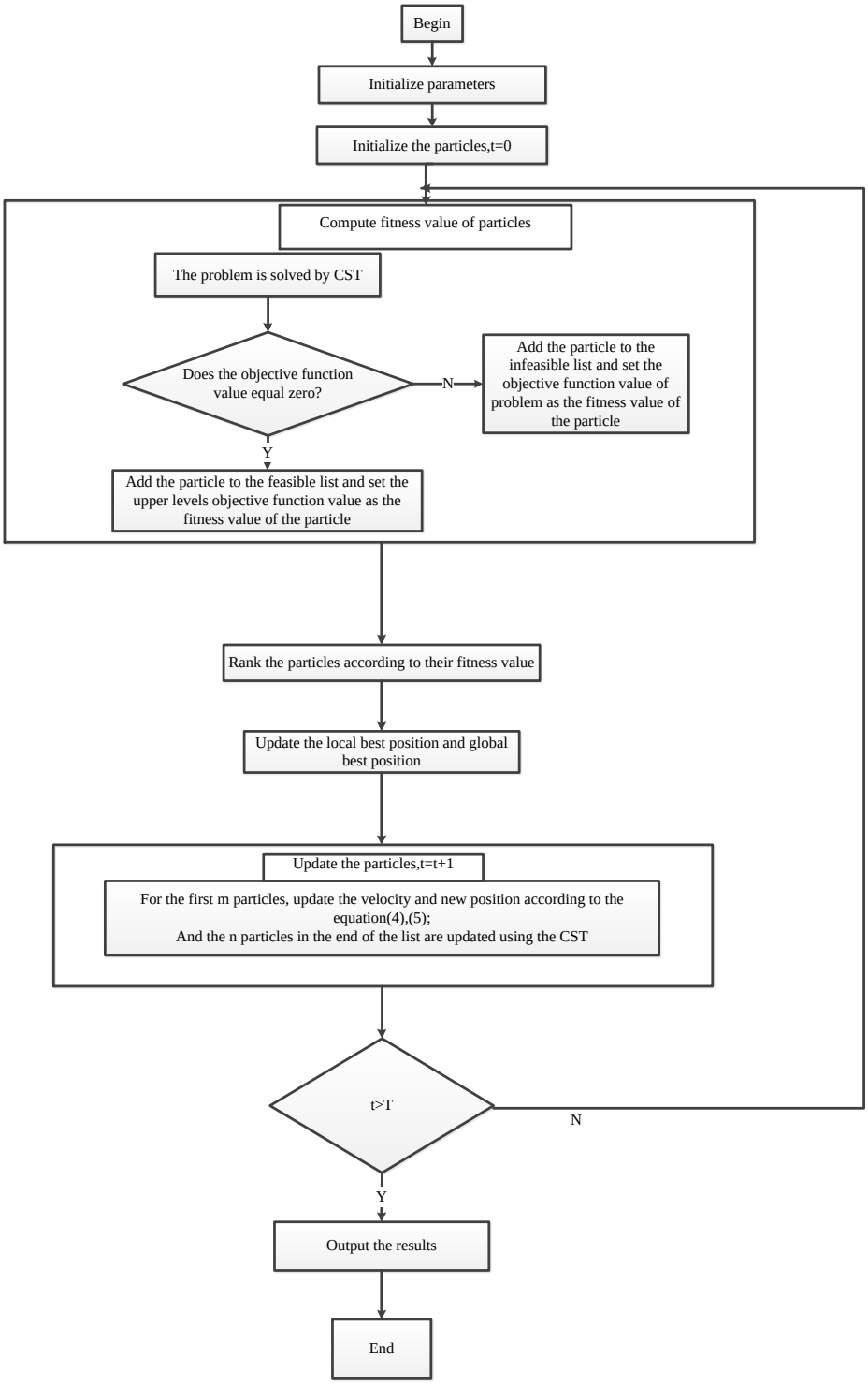

Fig4. The flow chart of the proposed hybrid intelligent algorithm

4. THE PROPOSED CSTPSO

A basic problem with the conventional PSO for the MPPT system can be traced to its random nature. It can be seen that the last two terms in (5) is totally dependent on random numbers. Two potential problems can be readily observed by investigating (5). First, during the exploring phase of algorithm (searching towards the *GP*), the particles change their positions (in this case duty cycle) based on the perturbation in the velocity. Therefore, if the change in duty cycle in two successive iterations is very low, the corresponding

change in array operating voltage will also be very low. Thus, more iteration is needed to reach the final solution. Second, the farther the particle from the best position (based on its own experience and its neighbor), a larger change in the velocity is required to follow the best position. However,too large change in the velocity might cause the particle to escape from the vicinity of the GP. This opens up the probability of converging to a local peak instead of the GP.However, both problems can be resolved by carefully observing the trends in P–V curves under partial shading and taking advantages of their properties described in Section 2. It is noted that the minimum distance between two consecutive peaks are displaced by 80% of the V_{oc} of the unshaded module. Thus, by removing the random factor in (5) and limiting the velocity factor (V_{max}) according to the distance between two peaks, the conventional PSO is transformed to a more deterministic structure. The key element of this transformation is the possibility of removing the random numbers in (5). Fittingly, the transformed equation is named as chaos searching technique PSO (CSTPSO). It can be seen that proposed modifications offers several advantages: 1) Due to the absence of randomness, the particles follow a deterministic behavior. Subsequently, for each independent run, the obtained final solution is consistent with respect to iteration size. In the conventional PSO, this iteration number (final solution's iteration) changes due to random number. 2) Tuning effort is greatly reduced; only one parameter i.e. the inertia weight, w, needs to be tuned. 3) The method significantly simplifies the optimization structure compared to the conventional PSO. It lessens the computation requirement and can be easily realized by a low cost microprocessor. 4) The limiting velocity factor, V_{max} , can be very useful in the variation of environmental conditions; one such example is in the tropical countries. The occurrences of clouds in tropical region are very common, resulting in frequent alterations in P–V curves. By manipulating the value of V_{max} , the values of duty cycles increase or decrease slowly in two successive MPPT cycles. Although, searching capability tends to be slower, the GP tracking is guaranteed.

5. THE CSTPSO MPPT

5.1. Direct Control Method

Fig.5 (a) shows a boost converter used in conjunction to a typical MPP controller. Fig.5(b) depicts the conventional MPP tracking scheme. Typically it consists of two independent control loops [26,27]. With regards to the ease of design, inexpensive maintenance and low cost solution, implementation is mostly done using PI controllers. However, due to the unpredictable environmental conditions and non-linear characteristics of PV system, the PI controllers tend to lose their performance when employed in PV system [28]. Alternatively, Fig. 5(c) shows the direct control scheme to track the *GP* [11].Both PI control loops are eliminated and duty cycle is computed directly in the MPP tracking algorithm. This scheme offers number of advantages: (1) it simplifies the hierarchy of the control structure, (2) reduces the computation time and (3) eliminates the need to tune the PI gains. In essence, it simplifies the implementation of the conventional PI-based MPPT tracking while maintaining the similar optimal results.

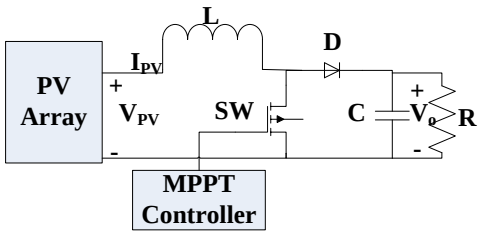

(a)

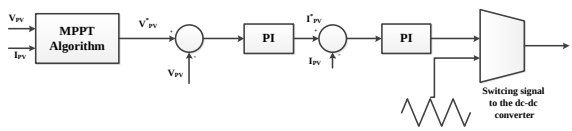

(b)

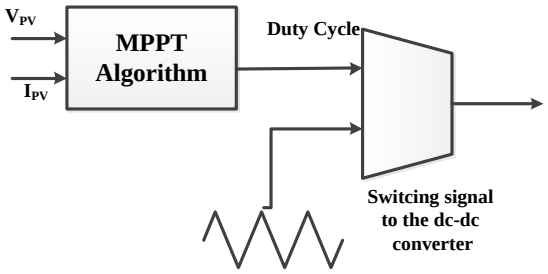

(c)

Fig. 5. (a) MPPT boost converter (b) conventional MPPT structure and (c) proposed direct control structure

5.2. Implementation of Proposed Method

To illustrate the application of CSTPSO to track the MPP using the direct control technique, a numerical example is used. First a solution vector of duty cycles with N_p particles is defined:

$$x_i^k = d_g = [d_1, d_2, d_3, ..., d_{NP}] \tag{8}$$

The objective function is chosen to be:

$$f(x_i^k) \; \rangle \; f(P_{best,i}) \tag{9}$$

The overall MPPT algorithm operates in two modes. Under normal condition, i.e. slow change in the environmental variation, the algorithm operates in local mode where it maintains the existing GP of the PV array. However, if partial shading occurs, the global mode is activated, i.e. the algorithm immediately jumps to the CSTPSO subroutine where the GP is computed. Once the GP is successfully located, the algorithm switches back to local mode. In this mode, hill climbing with variable step-size perturbation is employed.

5.3. Global Mode

To implement the CSTPSO, the following parameters are used: N_P=3 and ω=0.4. As discussed in section 3, during partial shading the PV curves are characterized by multiple peaks which are displaced with each other by an integral multiple of 80% of V_{oc} (n×0.8×Voc). The objective function is defined to be the output array power. Furthermore, V_{max} is chosen to be 0.035; this value ensures that no major peak is missed when the algorithm operates in the global mode. The velocity vector is initialized to zero. The range of the duty cycle is calculated using [15]:

$$d_{\min} = \frac{\sqrt{\eta_{bb} R_{L\min}}}{\sqrt{R_{PV\max}} + \sqrt{\eta_{bb} R_{L\min}}} \tag{10}$$

$$d_{\max} = \frac{\sqrt{\eta_{bb} R_{L\max}}}{\sqrt{R_{PV\min}} + \sqrt{\eta_{bb} R_{L\max}}} \tag{11}$$

where, η_{bb} is the converter efficiency of the converter, R_{Lmin} and R_{Lmax} are the minimum and maximum values of the connected load at the output, respectively. While, R_{PVmin} and R_{PVmax} are the reflective impedances of the PV array, respectively. Let's assume that initially the algorithm is settled at MPP (point A) as shown in Fig. 6 (a). Suddenly, a change in environmental condition occurs; it results in the reduction of the tracked power even though the duty cycle is not changed. Since CSTPSO is based on search optimization, in principle, it should be able to locate the GP for any type of P–V curve regardless of environmental variations. However, to differentiate between the change in uniform insolation and occurrence of partial shading, the following check is performed [15]:

$$\frac{I_{d3} - I_{d2}}{I_{d3}} \geq 0.1 \tag{12}$$

$$\frac{V_{d3} - V_{d2}}{V_{d3}} \geq 0.2 \tag{13}$$

The values "0.1" and "0.2" are selected based on the observation that I_{MPP} and V_{MPP} are about 90% and 80% of I_{SC} and V_{OC} of a single peak I–V curve, respectively. If the inequalities in (12) and (13) are fulfilled, the occurrence of partial shading is confirmed. Accordingly, proposed method switches to global mode– the CSTPSO algorithm is activated. It can be also noted that the evidence of shading in (12) and (13) are formulated based on the staircase structure of I–V curves in partial shading– the existence of staircase confirm the shading.

Therefore, the conditions in (12) and (13) are not restricted to only three particles. It can be increased to any number of particles, in which the detection of stairs should be the main objective. More details for the usage of (12) and (13) can be found out in [15]. To start the optimization process, the algorithm transmits three duty cycles d_i (i=1,2,3) to the power converter. In Fig. 6, d_1 , d_2 and d_3 are marked by triangular, circular and square points, respectively. These duty cycles are computed using (10) and (11) and serve as the P_{besti} in the first iteration. Among these, d_2 is the G_{best} that gives the best fitness value, as illustrated by Fig. 6 (a). In the second iteration, the resulting velocity is only due to the G_{best} term as the (P_{besti} –d (i)) factor in (5) is zero. Furthermore, it can be observed that d_1 and d_3 are too far from d_2 . This will result in a large change in v_1 and v_3 i.e. more than V_{max} . However, since V_{max} has been set to 0.035, the corresponding velocities are limited to this value. Additionally, the velocity of G_{best} for d_2 is zero. This is due to the fact that (*Gbest* -d (2)) factor in (5) is zero. Hence the duty cycle d_2 is unchanged. As a result, this particle will not contribute in the exploration process. To avoid such situation, a small perturbation in duty cycle is allowed to ensure the change in the fitness value, as depicted in Fig. 6 (b). It can be also seen that the change in array voltage does not exceed the minimum possible displacement between the two successive peaks i.e. 80% of V_{oc}_module . Fig.6(c) shows the particles movement in the third iteration. Due to the fact that all the duty cycles in the previous iteration attain improved objective function, the velocity direction of these particles is unchanged and subsequently they move towards G_{best} in the same direction. In this iteration, the operating power is not improved for the case of d_3 as compared to its previous P_{best3} . Thus, in the next iteration, previous d_3 still serves as the P_{best3} . In the fourth iteration, d_1 and d_2 arrive at the *GP* region having a very low value of velocity. In most applications, this velocity is sufficiently small enough such that the corresponding duty cycle can no longer improves the objective function. Thus, if any of the particle (d_i) does not exhibit further improvement in objective function and the difference between the voltage of this particle to the other particles (d_j , where i≠j) is sufficiently small, the *GP* region is assumed to be found –both d_i and d_j lie on the neighborhood of the *GP*. This scenario is illustrated in Fig. 6(d). Generally, the proposed method exhibits a very good performance by selecting N_P=3 and V_{max}=0.035. However, more accurate results can be achieved either by increasing N_P or decreasing V_{max} . Both options yield better results but at the expense of more number of iterations. It can be seen in Fig. 6(e) that when V_{max} is reduced to 0.02, the resulting transitions of particles are very small and final convergence towards the GP is very smooth.

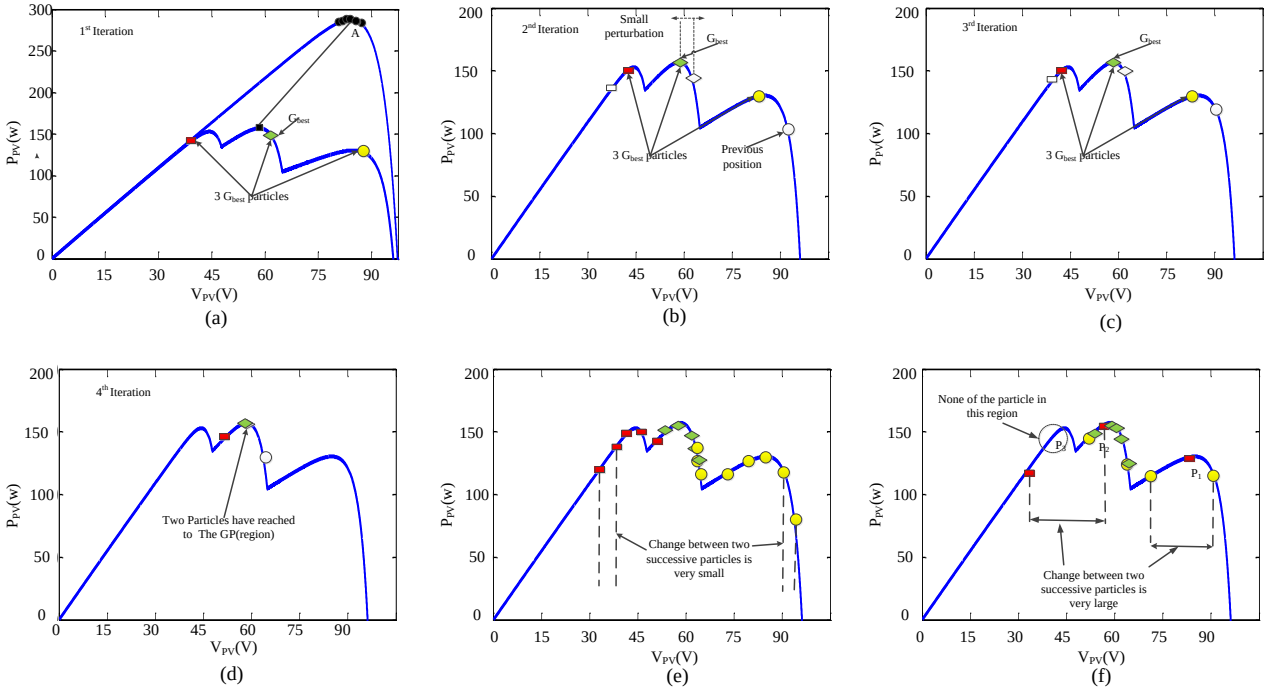

Fig. 6. Working principle of CSTPSO. (a) – (d) Particle movements in searching for the *GP*. (e) The effect of low value of V max . (f) The effect of large value of V_{max} .

Fig 6(f) illustrates the consequence of selecting a large value of V_{max} . When the optimization starts, the two extreme P_{best} particles (d_1 and d_3) are too far from G_{best} (d_2). In order for them to reach closer to d_2 , a large change in velocity is required. This is more crucial for d_3 ; it changes from 28V to 49V– more than 80% of V_{oc}_module . It has to be noted that despite the successful tracking of the *GP*, there exists areas in the P-V curve that could not be explored, due to the large change in array voltage. Such region is enclosed by the dotted lines in Fig. 6(f). If this region contains a higher peak than the previously found *GP*, the consequence would be that the final tracked MPP will be a local instead of the global. This important fact is highlighted by another numerical example, depicted in Fig. 7. The GP is located at the extreme left of the P–V curve. Among the first three duty cycles, d_1 turns out to be the G_{best}. Consequently, d_2 and d_3 require large change in duty cycles to move towards d_1 . It can be seen that this variation results in d_3 falling directly into the vicinity of a local peak. Hence the information on the *GP* is totally lost.

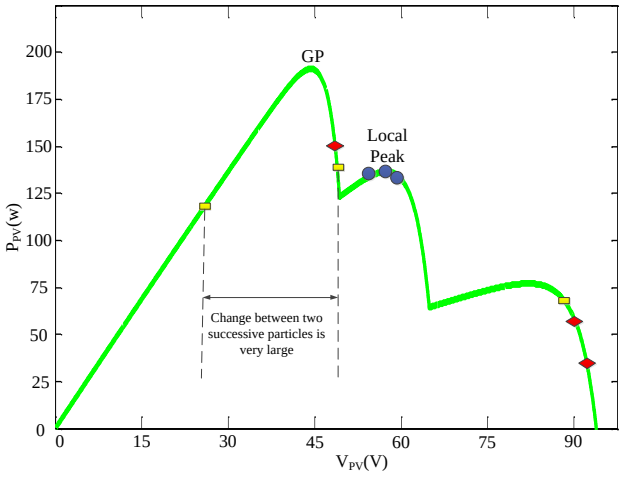

Fig. 7. Illustration of condition when the *GP* lies at the extreme P–V curve.

As a result, instead of searching the *GP*, the algorithm eventually tracks the local peak, resulting in lower power output from the PV array.

5.4. Global Mode

Because Once the GP is located, the algorithm exits the CSTPSO and switches to the local mode operation. In this mode, a conventional hill climbing (HC) method is employed. To minimize the energy loss due to oscillations in the vicinity of MPP, the variable step-size perturbation technique is applied.

The local mode is activated by either of the following conditions: 1) In the case of uniform insolation, the local mode is activated when inequalities (12) and (13) are not met. In the local mode, the best duty cycle (D_{ref}), which produces the maximum power, is used as a reference for the subsequent perturbation process. 2) The local mode is also activated once the stopping condition in the global mode is reached. The algorithm stops exploring the P–V curve and switches to local mode. The stopping condition occurs when the change in the velocity of any particle d_i , reaches a (predefined) small value and the difference between the voltages of d_i particle to the other particle (d_j ,where $i \neq j$) is sufficiently small. The difference could be selected between 30–60 percent of V_{oc} module . The resulting voltage due to d_i and d_j is relatively small which implies that both particles have successfully reached at the GP region. Fig.8 shows the complete flow chart of the proposed method that covers the operation in both global and local modes. In this flow diagram, if ΔP is greater than a certain threshold value (P_{thr}), then the tracking process starts to search for the new *GP* (in the main program).

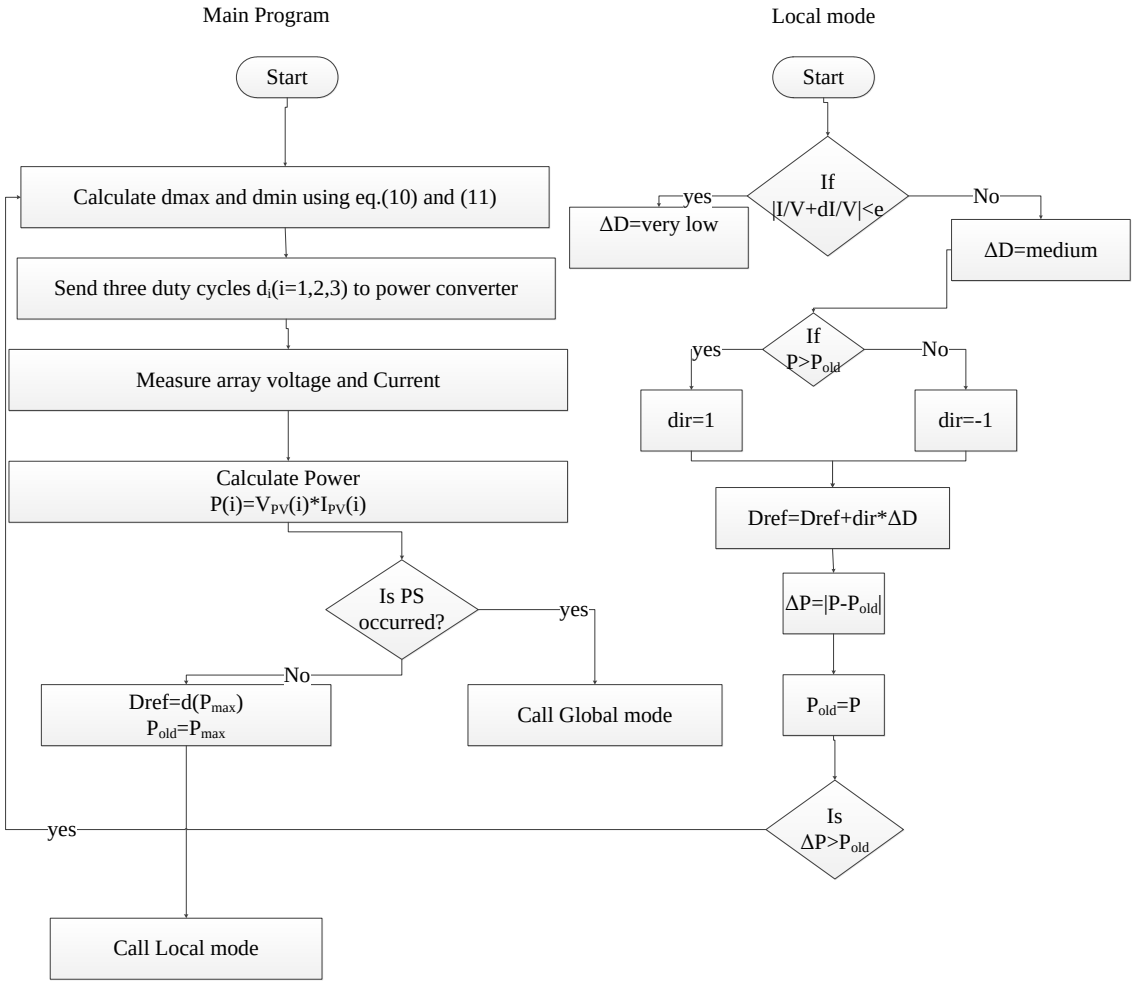

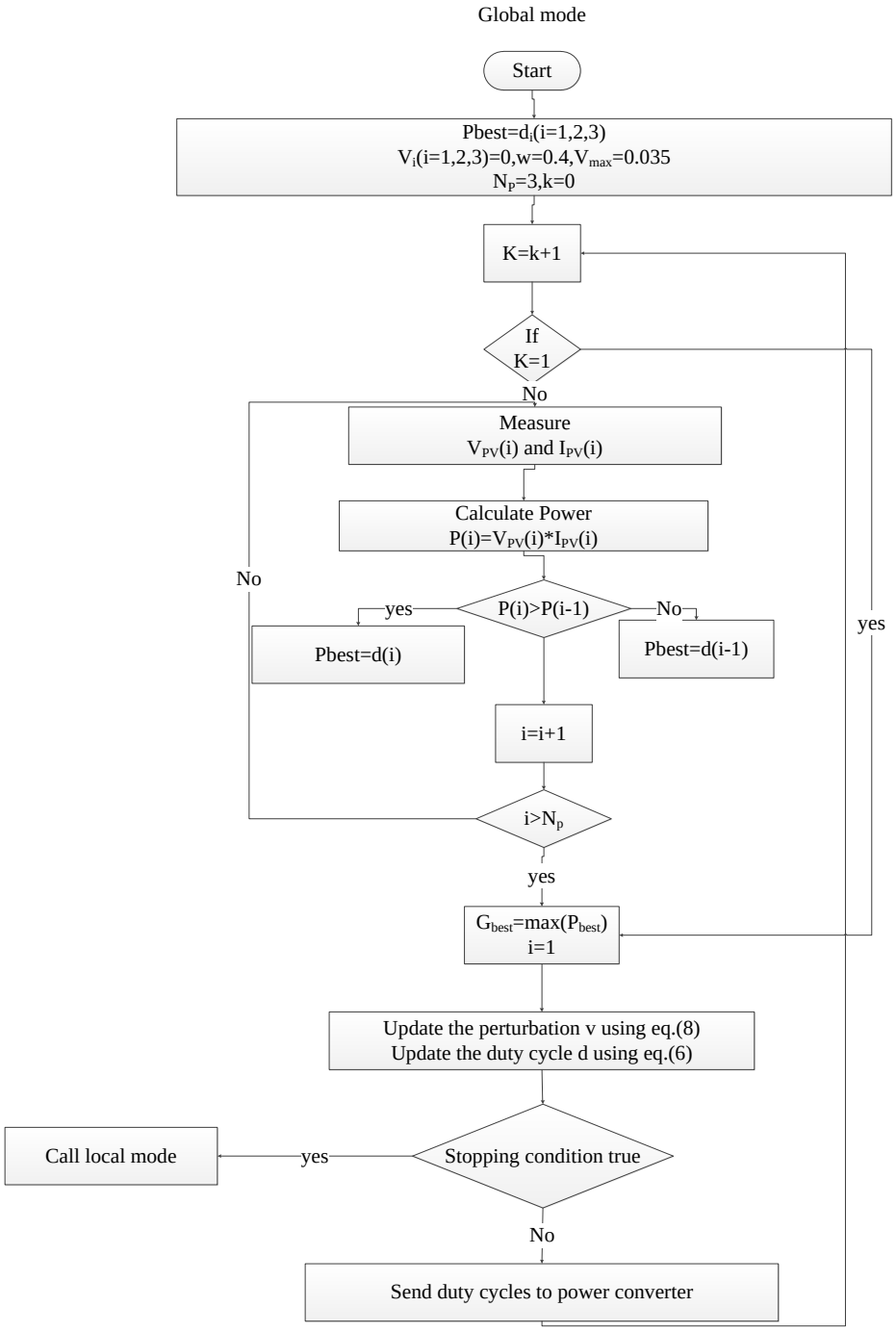

Fig. 8. Complete flow chart of the proposed MPPT method.

To determine ΔP, the array's output power at two different sampling instants,0.05 s apart, is considered. It was stated in [14] that the sudden variations in insolation are usually small in magnitude (smaller than G=0.027kW/m^2) and occurs within 1s. Based on this fact, (ΔG < 0.027 kW/m^2), P_{thr} can be fine-tuned accordingly. Moreover, the initial duty cycles (in this case three) for the power converter are selected between d_{min} and d_{max}. However, as stated earlier, the position of the duty cycle signals should be able to detect the staircase P–V curves during partial shading.

6. SIMULATION OF PROPOSED MPPT METHOD

6.1. Simulation Model

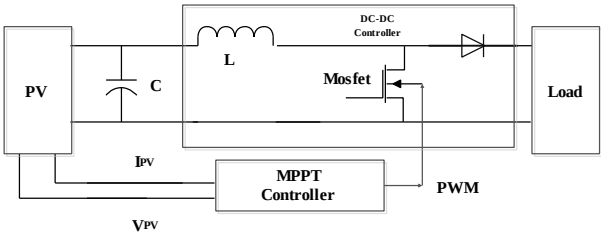

Fig.9. PV system with boost converter

Fig. 9 shows the simulation model for the converter with the MPPT implemented in this work. The following specifications for the boost converter are used: C_1=470μF, C_2=220μF and L=1mH. The converter switching frequency is set to 50 kHz. Furthermore, to ensure the system attains steady state before another MPPT cycle is initiated, the sampling interval is chosen as 0.05s. To evaluate the effectiveness of the tracking algorithm, the CSTPSO is compared with the conventional P&O method [9]. The P&O periodically updates the duty cycle d(k) by a fixed step-size with the direction of increasing power. Since, it was clear in section V that three particles can effectively track the GP; accordingly, this value will be used for simulation and hardware implementation. The Simulations are carried out using the comprehensive PV system simulator developed in [8].

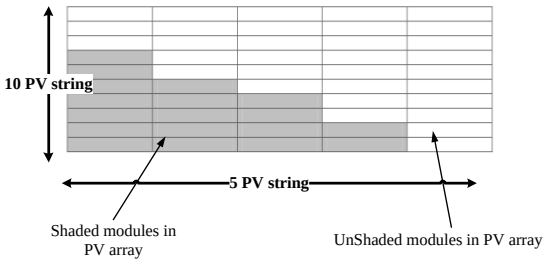

Fig. 10. 10× 5 PV array configuration with shading patterns

The PV array is connected in S-P configuration, which consists of five strings with ten modules per string. For simplicity, the array is represented in Fig. 10. Each block in the figure represents a PV module, rated (at STC) at P_{MAX} = 20W, I_{MPP}=1.21 A, V_{MPP}=16.8 V, I_{SC} =1.29 A, and V_{OC} =21V at *STC*. For the non shaded module, the full insolation is defined to be at 1000W/m^2 while the shaded receives 600W/m^2 (60% of insolation). An overall hypothetical shading pattern is suggested in Fig. 10.

6.2. Partial Shading simulation

Fig. 11 shows the resulting I–V and P–V curves for the two cases: (1) when the whole PV array attains full insolation, i.e. non-presence of Partial shading and (2) when the array is being partially shaded with the pattern shown in Fig. 10. It can be seen that the P–V curve for partial shading condition exhibits five local peaks labeled by A–E. Clearly, Peak E is the desired global maxima. These curves (cases 1 and 2) will be imposed on the CSTPSO (in simulation) to evaluate their respective Performances. The transition rate, i.e. the changes of one insolation level to another is set to 2s.

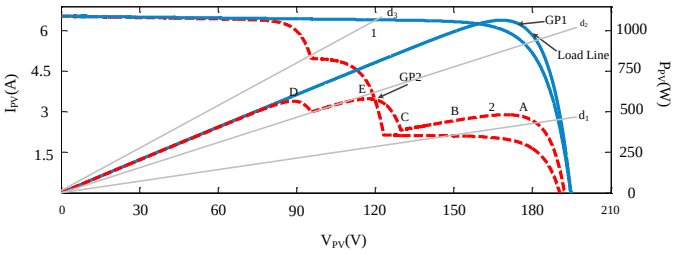

Fig 11. I–V and P–V curves used for testing of CSTPSO.

Fig. 12 shows the tracked voltage, current and duty cycle for CSTPSO. Initially, the PV array uniformly receives 50% of full insolation, i.e. 500W/m^2 . The operating power (P_{MPP}) is approximately 500 W, which corresponds to V_{MPP}=168V and I_{MP}=3A. At t=2 s, the insolation is stepped from 500W/m^2 to full insolation, i.e. 1000 W/m^2 . This action forces the CSTPSO algorithm to search for the new maximum operating power (GP_1) at P_{MPP}=1000 W. To cater for this change, the CSTPSO algorithm first transmits three duty cycles to the power converter at t=2 s to identify the insolation condition. This is shown by the variation in the duty cycle plot, d in Fig. 12.Using the computed values of these duty cycles and checking them with (12) and (13), the existence of uniform insolation is confirmed. Accordingly, at the fourth sampling cycle, it begins to search for the

global maxima using the local mode algorithm. It correctly tracks the corresponding GP_1 at V_{MPP}=168V and I_{MP}=6A within 8 sampling cycles. Furthermore, it can be observed that the steady state oscillation around GP_1 is very small due to the small perturbation step size, once the CSTPSO algorithm has located the MPP.

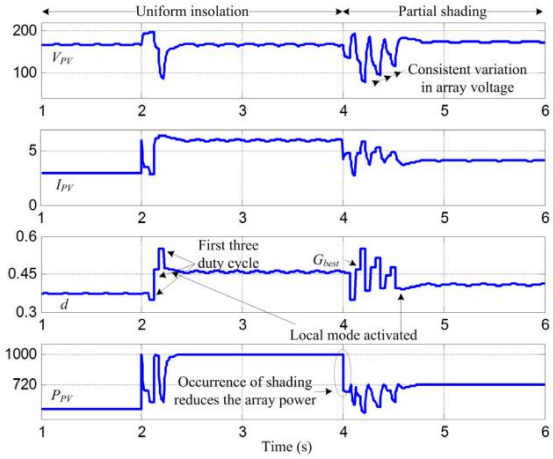

Fig. 12. Tracking voltage, current, duty cycle and power CSTPSO

At t=4s, the array is subjected to partial shading. For this condition the normal (single peak) P–V curve is replaced by the curves with multiple peaks (case 2). This in turn, changes the operating point from 1 to 2 as shown in Fig. 11. As before, the CSTPSO starts the tracking process by sending three duty cycles. Once the information obtained from (12) and (13) confirms the occurrence of partial shading, it kicks-in into the global mode algorithm. During the search for the GP, the exploration of P–V curves results in operating point fluctuations as can be clearly observed by the rapid variation in d as shown in Fig.12. At the ninth cycle, the CSTPSO algorithm successfully locates the new maxima, i.e. GP_2=722.4W, which corresponds to V_{MPP} = 172 V and I_{MP} = 4.2 A. Once GP_2 is found, the algorithm immediately switches to the local mode to maintain that operating point. It can also be seen that the fluctuations in operating voltage and current consistently decreases with the increment in iteration number. This can be attributed to the fact that the V_{max} factor does not allow the particles to move very fast towards the *GP*. For the case of P&O, when the operating point shifts from 1 to 2, it enters the vicinity of the local peak (point D). Since the previous sampled power P(k–1) is greater than current value P(k), the duty cycle decreases–causing the operating point moves toward the right side of MPP . However, in the next successive samples, if P(k–1) is found to be less than P(k), the operating point will move toward the right side of MPP .Eventually, the P&O algorithm will force the operating point to go forward and backward around point *D*, resulting in a sustainable oscillation around that point. Clearly the operating point will never be able leave the vicinity of point *D*, i.e. the algorithm is always trapped in local maxima.

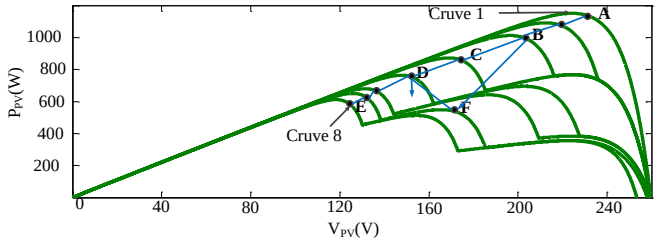

Fig. 13. Change in the PV characteristic

6.3. Tracking under slowly varying partial shading conditions

In certain environmental conditions, the shading can vary slowly [8]. Examples of such situation are sticking dirt and shadow from cloud. To emulate the slow shading condition, a set of 8 P–V curves are updated one by one at a transition rate of 7.5 minutes, as shown in Fig. 13. Both CSTPSO and P&O are evaluated under this gradual change in insolation and their tracking paths are shown in the same figure. It can be clearly seen that the CSTPSO follows the tracking path ABCDE, which tracks the *GP* for every P–V curve. On the other hand, the tracking path of P&O is seriously compromised; this is reflected by its transverse path (ABFD). In this path, for several P–V curves, P&O fails to track the

true *GP*, thus confirming the drawback of this method. Table I shows the comparison of the tracked energy and the array utilization of methods for the complete two hours testing duration(in simulation).It can be seen that the energy yield by the CSTPSO is exceptionally near to 100%. It is worth noting that the extracted power and energy yield with proposed CSTPSO will be much higher than other methods, if the difference in local peak and *GP* is higher and the shading continues for longer duration. Based on the simulation studies described above, the performance comparison between the proposed and existing methods is carried out and is given in table 1. Here tracking efficiency is calculated by taking the ratio between averaged output power obtained under steady state and maximum available power of the PV array under certain shading pattern in Figure 14 . This table clearly illustrates the superiority of the CSTPSO based algorithm in tracking the GMPP in comparison with the methods available in the literature.

6.4. Tracking under extreme partial shading

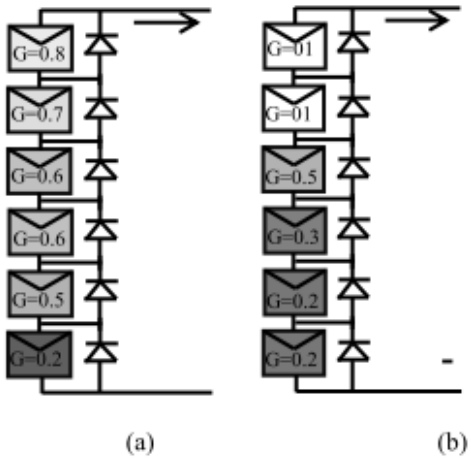

Fig. 14. 6S PV configuration a) Pattern-1, b) Pattern-2

The transition rate is set to 2s. It can be noted that the global peaks GP_2 and GP_3 lie at the right and left extreme of P–V curves, respectively. For the conventional MPPT method, if the new operating point (due to partial shading) is too far from the current GP, either of the following will results: (1) it will most likely being trapped at local peak [15] or (2) it will require many MPPT cycles to reach at GP [15]. For instance, in Fig. 15, due to the partial shading, when the PV array curve changes from curve 1 to 2, the operating point shifts from point A (previous) to A′ (present). If the P&O method is employed, the algorithm incrementally moves towards the MPP region and finally tracks a peak at the neighborhood of A′.

Table1. Comparison of the CSTPSO and PSO , P&O ,Fuzzy methods

Shading pattern	MPPT Method	Power (watt)	Voltage (volts)	Current (amperes)	Tracking Speed (seconds)	Array utilization
1	CSTPSO	52.2	83	0.628	5.05	99.80
	PSO	52.22	83.7	0.624	6.87	99.65
	P&O	26.76	106.2	0.252	2.02	51.23
	Fuzzy	49.76	98.5	0.598	6.97	99.54
2	CSTPSO	39.3	34	1.156	3.97	99.97
	PSO	39.3	33.8	1.163	10.02	99.95
	P&O	24.428	98.9	0.247	2.34	62.21
	Fuzzy	38.67	39.08	1.098	11.90	99.78

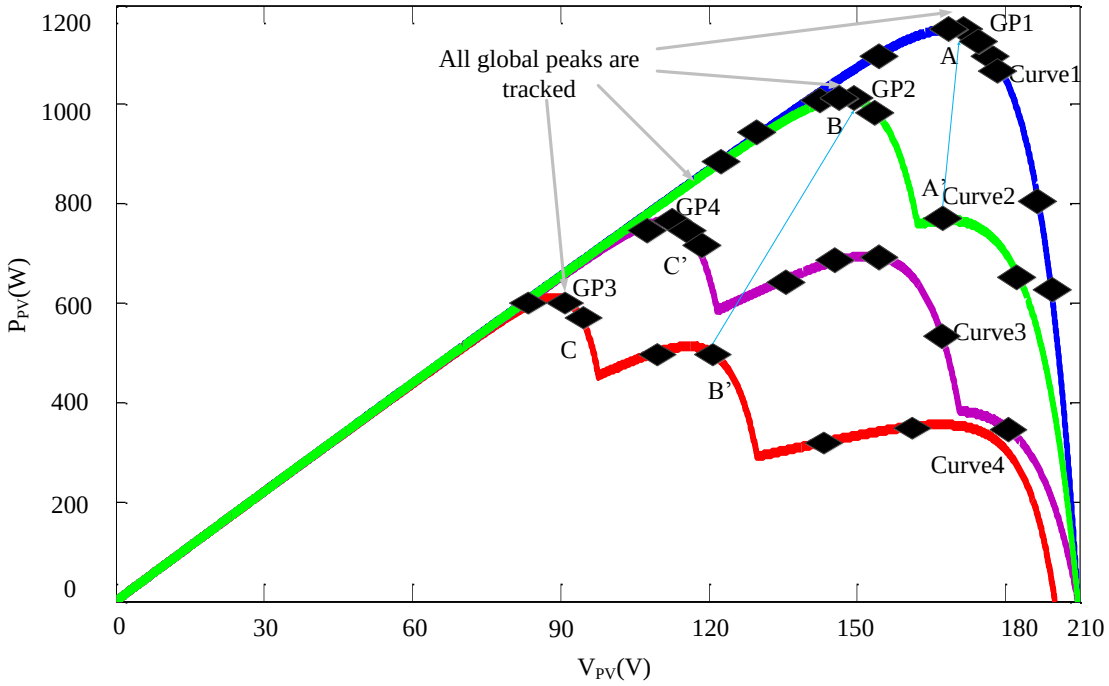

Fig. 15. P–V curves used to test the performance of the CSTPSO under the extreme partial shading conditions

However, it has no means of knowing whether the tracked MPP is a local or global peak. Clearly it is the former and it is worth noting that the difference in power between the two is 50W, i.e. 7% of the output power. This is a very significant loss for a PV system. For CSTPSO, when the operating point shifts from A to A', and once the algorithm realize the sudden reduction in power using (12) and (13), it immediately initiates the global mode. It begins the exploring phase of the CSTPSO. Thereafter, the movements of particles are marked by the triangular points on curve 2. It can be observed that the scattered particles cover all the major peaks on this curve and finally it reaches GP_2, i.e. point *B*. In the next case, another partial shading pattern (curve 3) is imposed; the operating point now shifts from B to B'. Note that the latter is very far from the MPP of curve 3 (GP_3). Despite this extreme condition, the CSTPSO again searches the new MPP and tracks GP_3 without any difficulty. Similar scenario can be observed when the operating point changes from *C* to *C'*; accordingly the CSTPSO searches for the peak in curve 4 and successfully tracks its MPP (GP_4) too. Furthermore, it can be noticed that for all the curves under simulation, *GP* exists in a certain region i.e. 60–180V. This also confirms the validity of eq. (11) and (12) for calculating d_{min} and d_{max} .

7. CONCLUSION

In this paper, a hybrid intelligent algorithm by combining particle swarm optimization with chaos searching technique (CSTPSO) structure, the proposed method offers remarkable accuracy and speed compared to conventional other methods. Furthermore, due to the simplicity of the proposed method, it can be easily implemented using a low-cost microcontroller. It overcomes the weaknesses of conventional direct control method particularly in partial shading conditions. Simulation results have shown that the proposed method outperforms the conventional method in terms of tracking performance under Several different irradiance conditions, including various patterns for partial shading.

REFERENCES

[1] Robert C.N. Pilawa-Podgurski, David J. Perreault, "*Submodule Integrated Distributed Maximum Power Point Tracking for Solar Photovoltaic Applications*," IEEE Tran. on Pow. Elec., vol. 28, no. 6, pp. 2957-2967, June 2013.

[2] L. Y. Seng, G. Lalchand, and G. M. Sow Lin, "*Economical, environmental and technical analysis of building integrated photovoltaic systems in Malaysia*," Energy Policy, vol. 36, no.6, pp. 2130–2142, June 2008.

[3] R. Kadri, J.P. Gaubert, G. Champenois, "*An Improved Maximum Power Point Tracking for Photovoltaic Grid-Connected Inverter Based on Voltage-Oriented Control*", Industrial Electronics, IEEE Transactions on, vol.58 .pp. 66-75,2011.

[4] Bilal, B . "*Implementation of Artificial Bee Colony algorithm on Maximum Power Point Tracking for PV modules*" , 8th International Symposium on Advanced Topics in Electrical Engineering (ATEE), 2013.

[5]Sankarganesh, R. Thangavel, S, "*Maximum power point tracking in PV system using intelligence based P&O technique and hybrid cuk converter*", International Conference on Emergin Trend in Science, Engineering and Technology (INCOSET), 2012.

[6] Koutroulis, E. ; Blaabjerg, F. Photovoltaics,, "*A New Technique for Tracking the Global Maximum Power Point of PV Arrays Operating Under Partial-Shading Conditions*",, IEEE Journal of vol 2 , Issue: 2, pp. 184 – 190,2013.

[7] Este, x, E.J. banez, V.M. Moreno, A. Pigazo, M. Liserre, A. Dell'Aquila, "*Performance Evaluation of Active Islanding-Detection Algorithms in Distributed-Generation Photovoltaic Systems: Two Inverters Case*", Industrial Electronics, IEEE Transactions on,vol 58 pp. 1185-1193,2011.

[8] L. Wuhua, H. Xiangning, Review of Nonisolated "*High-Step-Up DC/DC Converters in Photovoltaic Grid-Connected Applications*", Industrial Electronics, IEEE Transactions on, vol 58 pp. 1239-1250,2011.

[9] X. Huafeng, X. Shaojun, C. Yang, H. Ruhai, "*An Optimized Transformerless Photovoltaic Grid-Connected Inverter*", Industrial Electronics, IEEE Transactions on,vol 58 pp. 1887-1895,2011.

[10] N.A. Rahim, K. Chaniago, J. Selvaraj, "*Single-Phase Seven-Level Grid-Connected Inverter for Photovoltaic System*", Industrial Electronics, IEEE Transactions on, vol 58 pp.2435-2443,2011.

[11] Robert C.N. Pilawa-Podgurski, David J. Perreault, "*Submodule Integrated Distributed Maximum Power Point Tracking for Solar Photovoltaic Applications*" IEEE Tran. on Pow. Elec., vol. 28, no. 6, pp. 2957-2967, June 2013.

[12] Kinattingal Sundareswaran, Sankar Peddapati, and Sankaran Palani, " *MPPT of PV Systems Under Partial Shaded Conditions Through a Colony of Flashing Fireflies*," IEEE Transactions on energy conversion, Vol. 29, no. 2, pp.463-472, June 2014.

[13] N. Femia, G. Petrone, G. Spagnuolo, M. Vitelli, "*Optimization of perturb and observe maximum power point tracking method*", Power Electronics", IEEE Transactions on, vol 20 ,pp. 963-973,2007.

[14] A. Safari, S. Mekhilef, "*Simulation and Hardware Implementation of Incremental Conductance MPPT With Direct Control Method Using Cuk Converter*", Industrial Electronics, IEEE Transactions on, vol 58 pp.1154-1161,2011.

[15] Zhongping Wana, Guangmin Wangb, Bin Suna,, "*A hybrid intelligent algorithm by combining particle swarm optimization with chaos searching technique for solving nonlinear bilevel programming problems*", Swarm and Evolutionary Computation vol 8, pp. 26-32, February 2013.

[16] B.N. Alajmi, K.H. Ahmed, S.J. Finney, B.W. Williams, "*Fuzzy-Logic-Control Approach of a Modified Hill-Climbing Method for Maximum Power Point in Microgrid Standalone Photovoltaic System*", Power Electronics, IEEE Transactions on, vol 26 ,pp. 1022-1030,2011.

[17] Moacyr Aureliano, Luigi Galotto, Jr., Leonardo Poltronieri Sampaio, Guilherme de Azevedo e Melo and Carlos Alberto Canesin, " *Evaluation of the main MPPT Techniques for Photovoltaic Applications*" IEEE Transactions on Industrial Electronics, vol. 60, no.3, pp. 1156-1166, Mar. 2013.

[18] H. Patel, V. Agarwal, "*Maximum Power Point Tracking Scheme for PV Systems Operating Under Partially Shaded Conditions*", Industrial

Electronics, IEEE Transactions on, vol 55 pp. 1689-1698,2008.

[19] Bidyadhar Subudhi and Raseswari Pradhan," "*A Comparative Study on Maximum Power Point Tracking Techniques for Photovoltaic Power Systems*," IEEE Transactions on Sustainable Energy, vol. 4, no. 1, pp. 89-98, Jan. 2013.

[20] N. Tat Luat, L. Kay-Soon, " *A Global Maximum Power Point Tracking Scheme Employing DIRECT Search Algorithm for Photovoltaic Systems*", Industrial Electronics, IEEE Transactions on, vol 57, pp. 3456-3467,2008.

[21] E. Karatepe, T. Hiyama, M. Boztepe, M. Çolak, "*Voltage based power compensation system for photovoltaic generation system under partially shaded insolation conditions*", Energy Conversion and Management,vol 49 ,pp. 2307-2316,2008.

[22] B.N. Alajmi, K.H. Ahmed, S.J. Finney, B.W. Williams, "*A Maximum Power Point Tracking Technique for Partially Shaded Photovoltaic Systems in Microgrids*", Industrial Electronics, IEEE Transactions on, 2011.

[23] K. Ishaque, Z. Salam, "*An improved modeling method to determine the model parameters of photovoltaic (PV) modules using differential evolution (DE)* ", Solar Energy,vol 85 pp. 2349-2359,2011.

[24] K. Ishaque, Z. Salam, H. Taheri, A. Shamsudin, "*A critical evaluation of EA computational methods for Photovoltaic cell parameter extraction based on two diode model*", Solar Energy, vol 85 ,pp.1768-1779,2011.

[25] M. Miyatake, F. Toriumi, T. Endo, N. Fujii, "*A Novel maximum power point tracker controlling several converters connected to photovoltaic arrays with particle swarm optimization technique*", in: Power Electronics and Applications, European Conference on, pp. 1-10, 2007.

[26] V. Phimmasone, T. Endo, Y. Kondo, M. Miyatake, "*Improvement of the Maximum Power Point Tracker for photovoltaic generators with Particle Swarm Optimization technique by adding repulsive force among agents*", in: Electrical Machines and Systems,, pp. 1 – 6, 2009.

[27] V. Phimmasone, Y. Kondo, T. Kamejima, M. Miyatake, " *Evaluation of extracted energy from PV with PSO-based MPPT against various types of solar irradiation changes*", in: Electrical Machines and Systems (ICEMS), pp. 487 – 492, 2010.

[28] K. Ishaque, Z. Salam, H. Taheri, Syafaruddin, "*Modeling and simulation of photovoltaic (PV) system during partial shading based on a two-diode model*", Simulation Modelling Practice and Theory,vol 19 ,pp. 1613-1626,2011.

[29] R. Eberhart, J. Kennedy, "*A new optimizer using particle swarm theory, in: Micro Machine and Human Science*", MHS '95., Proceedings of the Sixth International Symposium on, pp. 39-43, 1995.

[30] Bader N. Alajmi, Khaled H. Ahmed, Stephen J. Finney, and Barry W. Williams, "*A Maximum Power Point Tracking Technique for Partially Shaded Photovoltaic Systems in Microgrids,"* IEEE Trans. on Industrial Electronics, vol. 60, no. 4, pp.1596-1606, April 2013.

[31] J. Young-Hyok, J. Doo-Yong, K. Jun-Gu, K. Jae-Hyung, L. Tae-Won, W. Chung-Yuen, "*A Real Maximum Power Point Tracking Method for Mismatching Compensation in PV Array Under Partially Shaded Conditions*", Power Electronics, IEEE Transactions on,vol 26 ,pp. 1001-1009,2011.

[32] K. Ishaque, Z. Salam, H. Taheri, "*Accurate MATLAB Simulink PV System Simulator Based on a Two-Diode Model*", Journal of Power Electronics,vol 11 pp. 9-18,2011.

[33] V. Zayats, "*Chaos searching algorithm for second order oscillatory system, in:Proceedings of the International Conference on Modern Problems of Radio Engineering*", Telecommunications and Computer Science, pp. 97–98, 2002.